

Figure 3 Effects of phosphorus addition on the diffusion-induced dislocation density, the activation energy of zinc diffusion, and the diffusion depth of zinc in GaP diffused at 850°C for 1 h.

of zinc helped by the existence of phosphorus vacancies is suppressed by the increase of phosphorus pressure. Consequently, the lattice distortion in GaP induced by the existence of interstitial zinc decreases.

It is thought that the increase of the activation energy and the decrease of the diffusion depth are due to both the decrease in phosphorus vacancies helping the interstitial diffusion of zinc, and of the short path diffusion of zinc along the dislocations.

References

- H. J. QUISSER, *Discuss. Faraday Soc.* **3** (1964) 305.
- M. L. JOSHI, *J. Electrochem. Soc.* **112** (1965) 912.
- J. BLACK and P. LUBLIN, *J. Appl. Phys.* **35** (1964) 2462.
- F. A. CUNNEL and C. E. GOOCH, *J. Phys. Chem. Solids* **15** (1960) 127.
- B. GOLDSTEIN, *Phys. Rev.* **118** (1960) 1024.
- S. PRUSSIN, *J. Appl. Phys.* **32** (1961) 1876.
- J. R. PATEL and A. R. CHAUDHURI, *ibid* **34** (1963) 2788.
- M. MARUYAMA, *Jap. J. Appl. Phys.* **7** (1968) 475.

Received 17 May
and accepted 19 July 1976

MASAHIRO KITADA
Central Research Laboratory
Hitachi Ltd,
Tokyo, 185,
Japan

Silicon cerium oxynitride

The existence of a new group of ceramics called the silicon metal oxynitrides was originally suggested by Jack [1]. In these materials the fundamental unit is the Si(O,N)₄ group; consequently, they are expected to be isomorphous with similar nitrides, silicates, and phosphates. This group of compounds can be further classified according to size and co-ordination chemistry of the metal ion. For cations similar in size to Si⁴⁺, substitution of the Si can occur. Thus, Al [2] and Be [3] can replace the Si in β-Si₃N₄, electrical neutrality being maintained by the appropriate substitution of oxygen for nitrogen atoms. Conversely, if the metal ion is much larger than the Si⁴⁺ ion, substitution cannot occur and the cation is restricted

to a position outside the Si(O,N)₄ group. For example, in the silicon lanthanide oxynitrides [4], all of the rare earth oxides examined to date form a compound of general formula Ln₄Si₂O₇N₂ (Ln = La, Sm, Y, Dy, Yb, and Er) which is isostructural with the silicates of the cuspidine-wohlerite series (cuspidine: Ca₄Si₂O₇F₂). Except for La, the above rare earth oxides also form a silicon oxynitride that is isostructural with the mineral Akermanite (Ca₂MgSi₂O₇). An exception to this general behaviour which has been observed for silicon cerium oxynitride is reported in this communication.

CeO₂* was dry mixed with Si₃N₄† in compositions ranging from 5 to 95 mol% CeO₂. Disc specimens (~5 g) prepared by cold compaction of the mixed powders were fired in a N₂ atmosphere

*99.99% purity, Research Chemicals, Phoenix, Arizona 85031.

†Advanced Materials Engineering, Ltd, Gateshead, UK.

TABLE I Observed and calculated diffraction data For Ce_3O_3N

<i>hkl</i>	<i>d</i>	Relative intensity	$Q_{obs.}$	$Q_{calc.}$
1 0 0	3.768	44	0.0704	0.0704
1 1 0	2.669	100	0.1404	0.1409
1 1 1	2.176	58	0.2112	0.2113
2 0 0	1.882	26	0.2823	0.2817
2 1 0	1.684	16	0.3526	0.3522
2 1 1	1.538	39	0.4228	0.4226

Cubic $a = 3.768 \text{ \AA}$

in the temperature range 1500 to 1750°C. The optimum temperature was found to be 1550°C, samples fired at higher temperature exhibiting severe weight losses (> 5%). The observed melting point was ~ 1550°C as in the $Si_3N_4-La_2O_3$ system [4]. It is noteworthy that CeO_2 behaved similarly, melting being accompanied by the apparent formation of a cerium oxynitride. In Table I, *d*-spacings for this phase (cubic $a = 3.768 \text{ \AA}$) are given. If it is assumed that the cerium is in the 3+ oxidation state, then one possible composition of this compound is Ce_3O_3N . Lines attributable to Ce_2O_3 were observed in the diffraction patterns of fired samples having a green composition of > 75 mol% CeO_2 ; however, no Ce_2O_3 was detected in the as-received CeO_2 . Thus, it is not unreasonable to assume that the cerium

present in the fired samples is in the normal 3+ oxidation state.

Examination of the diffraction patterns of the fired samples revealed, in addition to Ce_2O_3 lines, only one new set of peaks. The *d*-spacings, observed and calculated Q values ($Q = 4 \sin^2 \theta / \lambda^2$), and lattice parameters for this phase are shown in Table II. The diffraction pattern of this silicon cerium oxynitride can be indexed on the basis of an orthorhombic cell ($a = 7.256$, $b = 9.460$, $c = 4.184 \text{ \AA}$). It has not been possible to find another silicate with a similar crystal structure by comparison of lattice parameters as was done previously [5]. From the green compositions and assumption that the cerium is in the 3+ oxidation state, the composition of this new silicon cerium oxynitride is thought to be $3Ce_2O_3 \cdot 2Si_3N_4$. Thus, the behaviour of CeO_2 is in direct contrast to that of the other rare earth oxides which form compounds of the type $Ln_4Si_2O_7N_2$ and $Ln_2Si_3O_3N_4$ [4]. The reason for this difference is not yet known.

Acknowledgement

This work was supported in part under USAF Contract No. F33615-75-C-1005, and the work was conducted while Dr Wills was associated with Systems Research Laboratories, Inc, Dayton, Ohio, USA.

TABLE II Observed and calculated diffraction data for $3Ce_2O_3 \cdot 2Si_3N_4$

<i>hkl</i>	<i>d</i> (\AA)	Relative intensity	$Q_{obs.}$	$Q_{calc.}$
0 2 0	4.733	27	0.0446	0.0447
1 0 1, 2 0 0	3.630	79	0.0759	0.0760
1 1 1, 2 1 0	3.383	11	0.0874	0.0872
1 2 1, 2 2 0	2.882	100	0.1204	0.1207
0 4 0	2.366	17	0.1786	0.1788
0 0 2, 3 0 1	2.094	39	0.2281	0.2281, 0.2280
1 4 1, 2 4 0	1.981	26	0.2548	0.2549, 0.2548
0 2 2, 3 2 1	1.915	26	0.2727	0.2729, 0.2727
2 0 2, 4 0 0	1.814	15	0.3039	0.3041, 0.3040
2 2 2, 4 2 0	1.695	12	0.3481	0.3488, 0.3486
2 3 2, 4 3 0	1.573	7	0.4042	0.4047, 0.4045
3 1 2, 3 4 1	1.564	10	0.4088	0.4106, 0.4068
4 4 0, 2 6 0, 1 6 1	1.442	18	0.4809	0.4826, 0.4783, 0.4784
1 0 3, 4 0 2, 5 0 1	1.370	8	0.5328	0.5324, 0.5320, 0.5318
1 2 3, 4 2 2, 5 2 1	1.317	14	0.5765	0.5771, 0.5768, 0.5766

Orthorhombic $a = 7.257 \text{ \AA}$, $b = 9.460 \text{ \AA}$, $c = 4.184 \text{ \AA}$

References

1. K. H. JACK, *Trans. J. Brit. Ceram. Soc.* **72** (1973) 376.
2. K. H. JACK and W. I. WILSON *Nature, Phys. Sci.* **285** (1972) 28.
3. I. C. HUSEBY, H. L. LUKAS and G. PETZOW, *J. Amer. Ceram. Soc.* **54** (9-10) (1975) 361.
4. R. R. WILLS, R. W. STEWART, J. A. CUNNINGHAM and J. M. WIMMER, *J. Mater. Sci.* **11** (1976) 749.
5. R. R. WILLS, S. HOLMQUIST, J. M. WIMMER and J. A. CUNNINGHAM, *J. Mater. Sci.* **11** (1976) 1305.

Received 24 May

and accepted 25 June 1976

R. R. WILLS

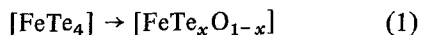
Battelle Columbus Laboratories,
505 King Avenue,
Columbus, Ohio, USA

J. A. CUNNINGHAM

Air Force Materials Laboratory,
Wright-Patterson Air Force Base, Ohio, USA*Association of iron microtraces with oxygen in tin chalcogenides*

A factor which affects the stabilization of the properties of thermoelectric materials of IV-VI semiconductors and the service life of thermoelectric generators is the diffusion of impurities from bridging materials, such as Fe in thermoelements. In addition to this, processes may occur between these doping elements and impurities which are inevitably present in the matrix. All these factors complicate considerably the picture of degradation of materials. In this work we demonstrate, by means of Mössbauer effect measurements, that in the IV-VI semiconductor subgroup of tin chalcogenides, one of which (SnTe) is used at the bridge-thermoelement interface, an association exists between iron and oxygen successively diffused in the matrix. Moreover, in the presence of traces of iron, the oxygen is not randomly distributed on the crystallographic sites.

Several studies of the ^{57}Fe stabilization forms in single lattices using the Mössbauer effect have been reported [1-5]. In some instances more than one state of charge has been identified and models for the stabilization form have been proposed. Fano and Ortalli [5] have reported that for Sn chalcogenides doped with Fe, different peaks are seen in the presence of doping elements such as oxygen which partially substitute tellurium in the lattice. Thus it can be assumed that the cluster formed by ^{57}Fe in an interstitial position with its neighbours $[\text{FeTe}_4]$, partially change into other forms such as:



with $x = 1, 2 \dots$, due to the oxidization effect.

In this work we attempt to ascertain if the existence of these clusters reflects a random distribution of oxygen in the various crystallographic sites of the single crystal, or if the substitution of oxygen for tellurium in the vicinity of the iron is due to the preference of the iron to associate itself with the oxygen.

To investigate this, measurements were made of the variation of the Mössbauer peak intensity corresponding to the various clusters with annealing time at 400°C in inert atmosphere. SnS and SnTe single crystals doped with microtraces of ^{57}Co were used and successively submitted to oxidation for 5 h at 400°C in an atmosphere of $\frac{1}{3}\text{O}_2$ and $\frac{2}{3}\text{N}_2$ were examined. The synthesis of the single crystals, the doping with ^{57}Co , the oxidation process and the measurement techniques are reported in [5], together with the typical spectrum of non-oxidized $\text{SnS}(^{57}\text{Fe})$ and $\text{SnTe}(^{57}\text{Fe})$ samples.

The homogeneous distribution of the transition elements in the samples was tested prior to oxidation, by comparing the spectrum intensity of that side of the sample side on which $^{57}\text{CoCl}_2$ was deposited with the spectrum intensity of the opposite side. ^{57}Co was considered to be homogeneously distributed throughout the sample when the two intensities were equal.

The spectrum of $\text{SnS}(^{57}\text{Fe})$ after the oxidation process is shown in Fig. 1a. The curve can be resolved into two quadrupole couplings (Q_1 and Q_2); Q_1 has the same Mössbauer parameters (δ , ΔE , $FWHM$) as the non-oxidized samples (see Table I). Any uncertainty in the computer fitting was removed using the following facts:

(1) all spectra obtained for samples oxidized at